PROCEEDINGS OF SCIENCE

Multiplicity Fluctuations in Relativistic Nucleus-Nucleus Collisions

Mark I. Gorenstein*

Bogolyubov Institute for Theoretical Physics, Kiev, Ukraine

We discuss the event-by-event multiplicity fluctuations in relativistic nucleus-nucleus collisions. Recent results of the transport and statistical approaches are presented and compared with existing data.

Correlations and Fluctuations in Relativistic Nuclear Collisions
July 7-9 2006
Florence, Italy

*Speaker.

PoS(CPOD2006)043

1. Introduction

The fluctuations in high energy particle and nuclear collisions are studied on an event-by-event basis: a given observable is measured in each collision event and the fluctuations are evaluated for the selected set of these events (see, e.g., reviews [1]). The statistical model has been successfully used to describe the data on hadron multiplicities in relativistic A+A collisions (see, e.g., Ref. [2, 3, 4]). The fluctuations can be closely related to phase transitions in QCD matter, with specific signatures for 1-st and 2-nd order phase transitions as well as for the critical point [5, 6, 7].

2. HSD and UrQMD Transport Approaches

Only recently, due to a rapid development of experimental techniques, first measurements of particle multiplicity fluctuations in A+A collisions were done [8]. We start our discussion with the HSD [9] and UrQMD [10] transport approaches. More details are presented in Ref. [11]. The Fig. 1 presents the HSD and UrQMD results and the NA49 data points for the scaled variances of negatively, positively, and all charged particles in Pb+Pb collisions at 158 AGeV. The average values $\langle N_i \rangle \quad (i = +, -, ch)$ and variances $Var(N_i) \equiv \langle N_i^2 \rangle - \langle N_i \rangle^2$ are calculated for the samples of collision events with fixed number of projectile participants. The scaled variances are $\omega_i \equiv Var(N_i)/\langle N_i \rangle$. Note that $\omega = 1$ for the Poisson multiplicity distribution.

The final particles in the HSD and UrQMD simulations are accepted at rapidities $1.1 < y < 2.6$ (we use particle rapidities in the Pb+Pb c.m.s. frame) in accord to the NA49 transverse momentum filter. The HSD and UrQMD simulations both show flat ω_i values, $\omega_- \approx \omega_+ \approx 1.2$, $\omega_{ch} \approx 1.5$, and exhibit almost no dependence on N_P^{proj}. The NA49 data, in contrast, exhibit maximums, $\omega_- \approx \omega_+ \approx 2$ and $\omega_{ch} \approx 3$, for $N_P^{proj} \approx 50$, and a rather strong dependence on N_P^{proj}.

The Fig. 1 also shows results of the HSD and UrQMD simulations for the full 4π acceptance for final particles, and shows the NA49-like acceptance in the mirror rapidity interval, $-2.6 < y < -1.1$ of the target hemisphere. HSD and UrQMD both result in large values of ω_i, i.e. large fluctuations in the backward hemisphere: in the backward rapidity interval $-2.6 < y < -1.1$ (target hemisphere) the fluctuations are much larger than those calculated in the forward rapidity interval $1.1 < y < 2.6$ (projectile hemisphere, where the NA49 measurements have been done). Even larger fluctuations follow from the HSD and UrQMD simulations for the full acceptance of final particles.

The HSD and UrQMD results raise two questions: 1). What is the origin of strong fluctuations (ω_i is much larger than 1) within the HSD and UrQMD simulations both in the full acceptance and in the target hemisphere? 2). Why are no large fluctuations observed in the HSD and UrQMD simulations in the NA49 acceptance, i.e. within the projectile hemisphere?

In each A+A event only a fraction of all $2A$ nucleons (the participant nucleons) interact. We denote the number of participant nucleons from the projectile and target nuclei as N_P^{proj} and N_P^{targ}, respectively. The trivial geometrical fluctuations due to impact parameter variations usually dominate in high energy A+A collisions and mask the fluctuations of interest. It appears that even with the rigid centrality trigger, $N_P^{proj} = const$, used by NA49 Collaboration, the number of nucleon participants still fluctuates considerably. In each sample the number of target participants fluctuates around its mean value, $\langle N_P^{targ} \rangle \approx N_P^{proj}$, with the variance $V(N_P^{targ}) \equiv \langle (N_P^{targ})^2 \rangle - \langle N_P^{targ} \rangle^2$. The crucial point is that by this event selection one introduces an asymmetry between projectile and target

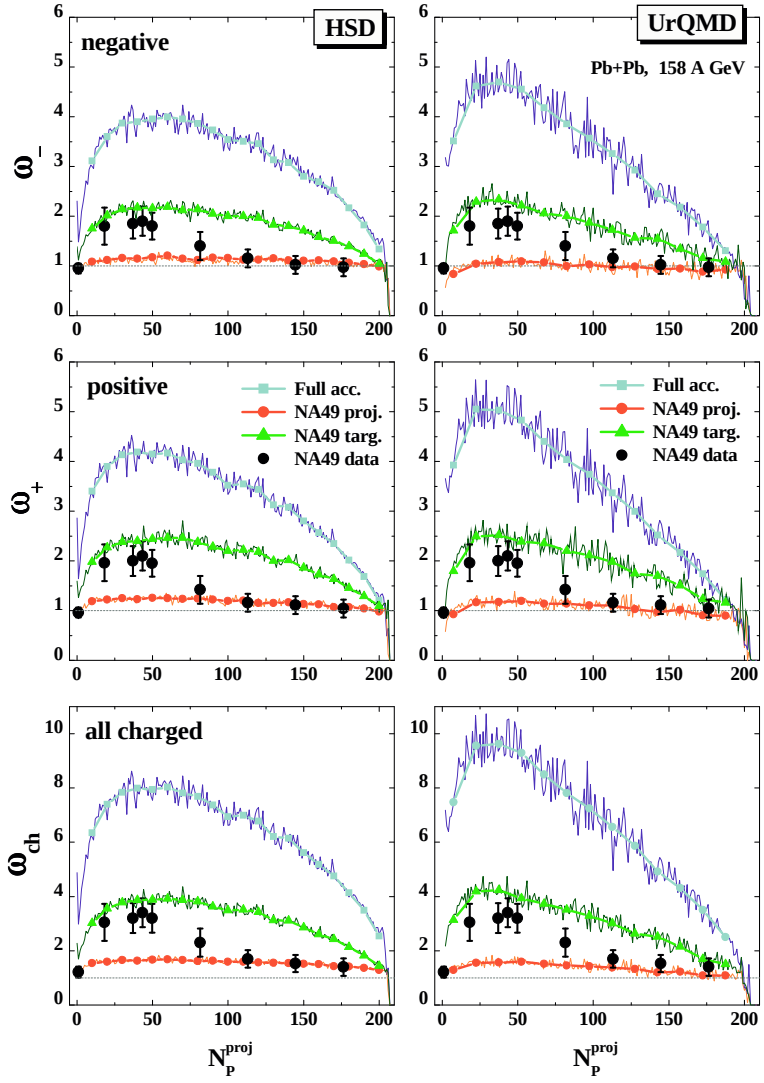

Figure 1: The results of the HSD (left) and UrQMD (right) simulations are shown for ω_-, ω_+, and ω_{ch} in Pb+Pb collisions at 158 AGeV as functions of N_P^{proj}. The black points are the NA49 data. The different lines correspond to the model simulations with the original NA49 acceptance, $1.1 < y < 2.6$, in the projectile hemisphere (lower lines), the NA49-like acceptance in the mirror rapidity interval, $-2.6 < y < -1.1$, in the target hemisphere (middle lines), and full 4π acceptance (upper lines).

participants. The number of projectile participants is constant by construction, whereas the number of target participants fluctuates. The consequences of this asymmetry depend on dynamics or properties of the model, respectively. The Fig. 2 presents the scaled variance $\omega_P^{targ} = V(N_P^{targ})/\langle N_P^{targ}\rangle$ calculated within the HSD and UrQMD models as the function of N_P^{proj}. The fluctuations of N_P^{targ} are quite strong: the largest value of $\omega_P^{targ} = 3 \div 3.5$ occurs at $N_P^{proj} = 20 \div 30$. The scaled variance ω_P for the total number of participants is easily found, $\omega_P = \omega_P^{targ}/2$, as $N_P = N_P^{targ} + N_P^{proj}$ and only a half of the total number, N_P, of participants, i.e., N_P^{targ}, does fluctuate. The scaled variances,

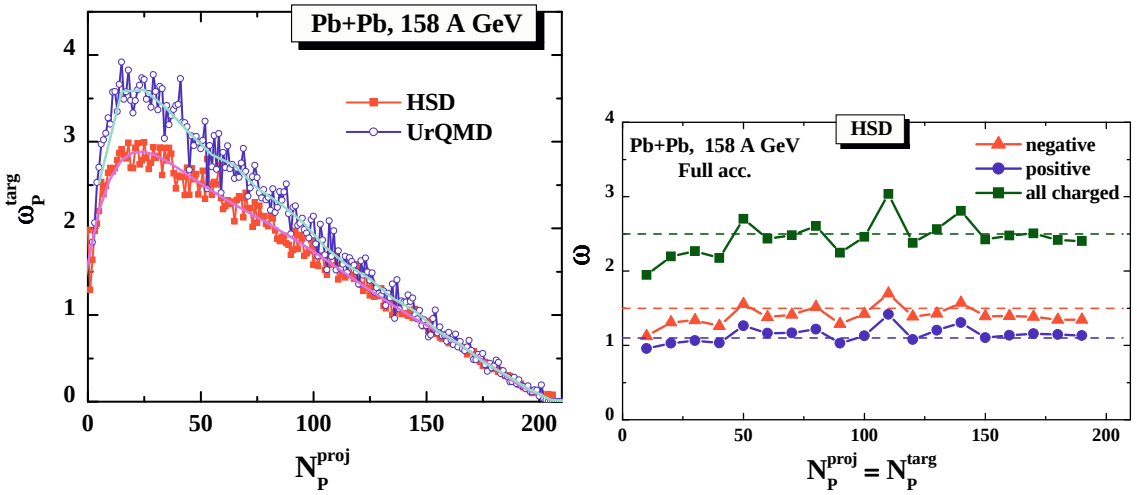

Figure 2: *Left* HSD and UrQMD simulations show similar scaled variances ω_P^{targ} as a function of N_P^{proj}. *Right.* The circles, triangles, and boxes are the results of the HSD simulations for ω_i in full 4π acceptance with $N_P^{targ} = N_P^{proj}$. This condition yields, $\omega_P^{targ} = 0$, and Eq. (2.1) is reduced to $\omega_i = \omega_i^*$. The dashed lines correspond to the HSD results for ω_i^* per N+N collision at 158 GeV: $\omega_{ch}^* = 2.5$, $\omega_-^* = 1.5$, $\omega_+^* = 1.1$.

ω_i , can be presented as:

$$\omega_i \;=\; \omega_i^* \;+\; \frac{1}{2}\,\omega_P^{targ}\,n_i \;, \tag{2.1}$$

where the fluctuations from one source is, ω_i^*, and the contribution due to the fluctuations of the number of sources, $\omega_P n_i$. The Fig. 2 (right) shows the HSD results with fixed target participant number, $N_P^{targ} = N_P^{proj}$. The ω_i become much smaller. This is due to the fact that terms proportional to ω_P^{targ} in Eq. (2.1) do not contribute, and ω_i become approximately equal to ω_i^*. The particle number fluctuations in the target hemispheres are much stronger (see Fig. 3, left) than those in the projectile hemispheres. Different models of hadron production in relativistic A+A collisions can be divided into three limiting groups: transparency, mixing, and reflection models (see Ref. [12]). The first group assumes that the final longitudinal flows of the hadron production sources related to projectile and target participants follow in the directions of the projectile and target, respectively. We call this group of models transparency models. If the projectile and target flows of hadron production sources are mixed, we call these models the mixing models. Finally, one may even speculate that the initial flows are reflected in the collision process. The projectile related matter then flows in the direction of the target and the target related matter flows in the direction of the projectile. This class of models we call the reflection models. The rapidity distributions resulting from the T-, M-, and R-models are sketched in Fig. 3 (right). An asymmetry between the projectile and target participants introduced by the experimental selection procedure can be used to distinguish between projectile related and target related final state flows of hadron production sources as suggested in Ref. [12].

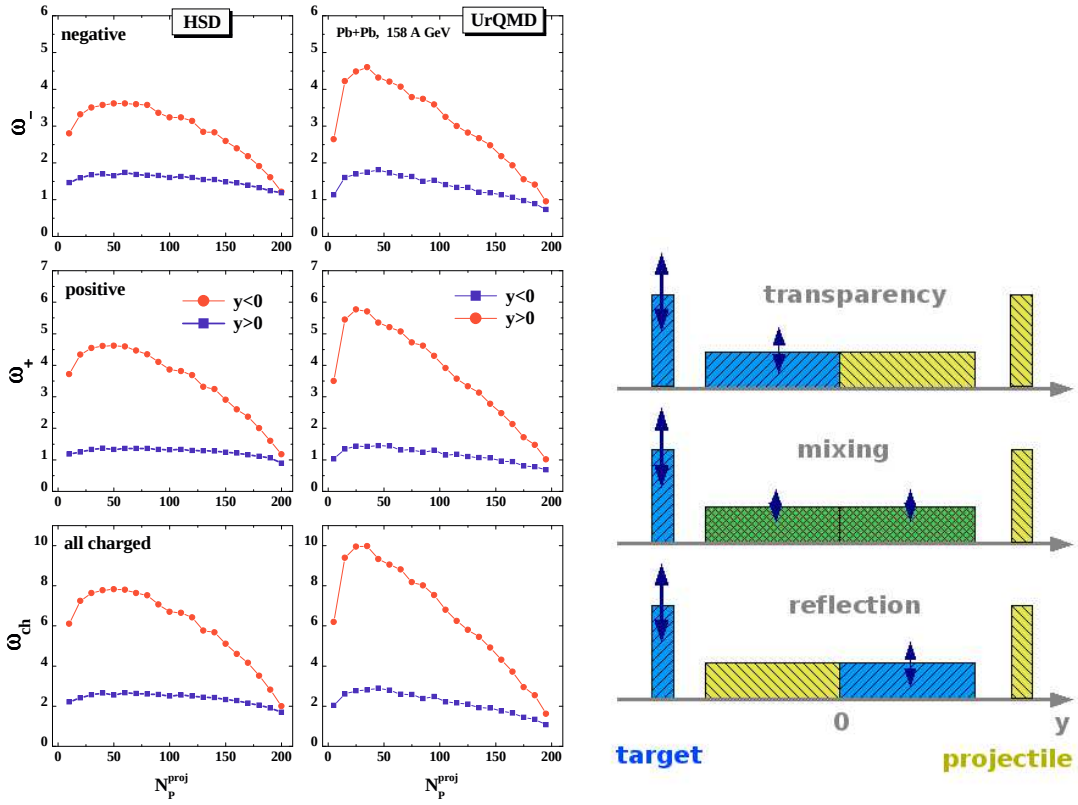

Figure 3: *Left.* The scaled variances ω_i for the projectile (boxes) and target (circles) hemispheres in the HSD and UrQMD simulations. *Right.* The rapidity distributions of the particle production sources in nucleus-nucleus collisions resulting from transparent, mixing, and reflection models (see Ref. [12] for details).

3. Multiplicity Fluctuations in Statistical Models

The mean multiplicities of positively, negatively and all charged particles are:

$$\langle N_- \rangle \;=\; \sum_{i,q_i<0} \langle N_i \rangle \;,\;\; \langle N_+ \rangle \;=\; \sum_{i,q_i>0} \langle N_i \rangle \;,\;\; \langle N_{ch} \rangle \;=\; \sum_{i,q_i\neq 0} \langle N_i \rangle \;, \tag{3.1}$$

where the average final state (after resonance decays) multiplicities $\langle N_i \rangle$ are equal to:

$$\langle N_i \rangle \;=\; \langle N_i^* \rangle + \sum_R \langle N_R \rangle \langle n_i \rangle_R \;. \tag{3.2}$$

In Eq. (3.2), N_i^* denotes the number of stable primary hadrons of species i, the summation $\sum_R$ runs over all types of resonances R, and $\langle n_i \rangle_R \equiv \sum_r b_r^R n_{i,r}^R$ is the average over resonance decay channels. The parameters b_r^R are the branching ratios of the r-th branches, $n_{i,r}^R$ is the number of particles of species i produced in resonance R decays via decay mode r. The index r runs over all decay channels of resonance R, with the requirement $\sum_r b_r^R = 1$. Note that different branches are defined in a way that final states with only stable hadrons are counted. To make a correspondence with NA49 data, both strong and electromagnetic decays of resonances should be taken into account.

In the GCE formulation of the hadron-resonance gas model the mean number of stable primary particles, $\langle N_i^* \rangle$, and the mean number of resonances, $\langle N_R \rangle$, can be calculated as:

$$\langle N_j \rangle \equiv \sum_{\mathbf{p}} \langle n_{\mathbf{p},j} \rangle = \frac{g_j V}{2\pi^2} \int_0^\infty p^2 dp \, \langle n_{\mathbf{p},j} \rangle \,, \tag{3.3}$$

where V is the system volume and g_j is the degeneracy factor of particle of species j (number of spin states). In the thermodynamic limit, $V \to \infty$, the sum over momentum states can be transformed into a momentum integral. The occupation numbers, $n_{\mathbf{p},j}$, of single quantum states (with fixed projection of particle spin) are equal to $n_{\mathbf{p},j} = 0, 1, \ldots, \infty$ for bosons and $n_{\mathbf{p},j} = 0, 1$ for fermions. Their average values, fluctuations, and correlations are the following:

$$\langle n_{\mathbf{p},j} \rangle = \frac{1}{\exp\left[\left(\varepsilon_{\mathbf{p}j} - \mu_j\right)/T\right] - \gamma_j} \,, \tag{3.4}$$

$$\langle (\Delta n_{\mathbf{p},j})^2 \rangle \equiv \langle (n_{\mathbf{p},j} - \langle n_{\mathbf{p},j} \rangle)^2 \rangle = \langle n_{\mathbf{p},j} \rangle \left(1 + \gamma_j \langle n_{\mathbf{p},j} \rangle\right) \equiv v_{\mathbf{p},j}^2 \,, \tag{3.5}$$

$$\langle \Delta n_{\mathbf{p},i} \Delta n_{k,j} \rangle_{g.c.e.} = v_{\mathbf{p},j}^2 \, \delta_{ij} \, \delta_{\mathbf{pk}} \,, \tag{3.6}$$

where T is the system temperature, m_j is the mass of particles of species j, $\varepsilon_{\mathbf{p}j} = \sqrt{\mathbf{p}^2 + m_j^2}$ is a single particle energy and γ_j referrs to quantum statistics ($+1$ and -1 for bosons and fermions, respectively, while $\gamma_j = 0$ gives the Boltzmann approximation). The chemical potential μ_j of species j equals to: $\mu_j = q_j \, \mu_Q + b_j \, \mu_B + s_j \, \mu_S$, where q_j, b_j, s_j are its electric charge, baryon number, and strangeness, respectively, while μ_Q, μ_B, μ_S are the corresponding chemical potentials which regulate the average values of these global conserved charges in the GCE. There are no correlations between different particle species, $i \neq j$, and/or between different momentum states, $\mathbf{p} \neq \mathbf{k}$. Only Bose enhancement, $v_{\mathbf{p},j}^2 > \langle n_{\mathbf{p},j} \rangle$ for $\gamma_j = 1$, and Fermi suppression, $v_{\mathbf{p},j}^2 < \langle n_{\mathbf{p},j} \rangle$ for $\gamma_j = -1$, exist for fluctuations of primary particles in the GCE.

The above equations correspond to the GCE. In the limit $V \to \infty$, Eq. (3.3) for the average multiplicities is also valid for both the CE and MCE, if energy density and conserved charge densities are the same in all three ensembles. This is usually referred to as the thermodynamical equivalence of all statistical ensembles. However, the thermodynamical equivalence does not apply to fluctuations [13, 14]. Multiplicity fluctuations can be quantified by the scaled variance. For negatively, positively, and all charged particles the scaled variances read:

$$\omega^- = \langle (\Delta N_-)^2 \rangle / \langle N_- \rangle \,, \quad \omega^+ = \langle (\Delta N_+)^2 \rangle / \langle N_+ \rangle \,, \quad \omega^{ch} = \frac{\langle (\Delta N_{ch})^2 \rangle}{\langle N_{ch} \rangle} \,. \tag{3.7}$$

The variances can be presented as a sum of the correlators:

$$\langle (\Delta N_-)^2 \rangle = \sum_{i,j;\; q_i<0, q_j<0} \langle \Delta N_i \Delta N_j \rangle \,, \quad \langle (\Delta N_+)^2 \rangle = \sum_{i,j;\; q_i>0, q_j>0} \langle \Delta N_i \Delta N_j \rangle \,,$$
$$\langle (\Delta N_{ch})^2 \rangle = \sum_{i,j;\; q_i\neq 0, q_j\neq 0} \langle \Delta N_i \Delta N_j \rangle \,, \tag{3.8}$$

where $\Delta N_i \equiv N_i - \langle N_i \rangle$. These correlators include both the correlations between primordial hadrons and those of final state hadrons due to the resonance decays. In the GCE the final state correlators can be calculated as [15]:

$$\langle \Delta N_i \Delta N_j \rangle_{g.c.e.} = \langle \Delta N_i^* \Delta N_j^* \rangle_{g.c.e.} + \sum_R \left[\langle \Delta N_R^2 \rangle \langle n_i \rangle_R \langle n_j \rangle_R + \langle N_R \rangle \langle \Delta n_i \Delta n_j \rangle_R \right] \,, \tag{3.9}$$

where $\langle \Delta n_i \, \Delta n_j \rangle_R \equiv \sum_r b_r^R n_{i,r}^R n_{j,r}^R \, - \, \langle n_i \rangle_R \langle n_j \rangle_R$.

The correlators in Eq. (3.9) can be presented in terms of microscopic correlators (3.6):

$$\langle \Delta N_i^* \, \Delta N_j^* \, \rangle_{g.c.e.} \, = \, \sum_{\mathbf{p},\mathbf{k}} \, \langle \Delta n_{\mathbf{p},i} \, \Delta n_{\mathbf{k},j} \rangle_{g.c.e.} \, = \, \delta_{ij} \, \sum_{\mathbf{p}} \, v_{\mathbf{p},j}^2 \, . \tag{3.10}$$

In the case of $i = j$ the above equations give the primordial scaled variances in the GCE. For chemical freeze-out conditions in heavy-ion collisions, the Bose effects for pions and resonance decay correlations dominate and lead to (see Ref. [14]): $\omega_{g.c.e.}^- \cong 1.1$, $\omega_{g.c.e.}^+ \cong 1.2$, and $\omega_{g.c.e.}^{ch} \cong 1.4 \div 1.6$, at SPS energies.

In the MCE, the energy and conserved charges are fixed exactly for each microscopic state of the system. This leads to two modifications in a comparison with the GCE. Firstly, the primordial microscopic correlators in the MCE become more complicated. The additional terms reflect the (anti)correlations between different particles, $i \neq j$, and different momentum levels, $\mathbf{p} \neq \mathbf{k}$. They appear due to exact charge conservations in the CE, or both charge and energy conservations in the MCE. (see also Ref. [14] for the CE),

$$\begin{aligned} \langle \Delta n_{\mathbf{p},i} \Delta n_{\mathbf{k},j} \rangle_{m.c.e.} &= v_{\mathbf{p},i}^2 \, \delta_{ij} \, \delta_{\mathbf{pk}} - v_{\mathbf{p},i}^2 v_{\mathbf{k},j}^2 \, |A|^{-1} [q_i q_j M_{qq} + b_i b_j M_{bb} + s_i s_j M_{ss} \\ &+ (q_i s_j + q_j s_i) \, M_{qs} - (q_i b_j + q_j b_i) \, M_{qb} - (b_i s_j + b_j s_i) \, M_{bs} + \varepsilon_{\mathbf{p}i} \varepsilon_{\mathbf{k}j} M_{\varepsilon\varepsilon} \\ &- (q_i \varepsilon_{\mathbf{p}j} + q_j \varepsilon_{\mathbf{k}i}) \, M_{q\varepsilon} \, + (b_i \varepsilon_{\mathbf{p}j} + b_j \varepsilon_{\mathbf{k}i}) \, M_{b\varepsilon} - (s_i \varepsilon_{\mathbf{p}j} + s_j \varepsilon_{\mathbf{k}i}) \, M_{s\varepsilon}] \, , \end{aligned} \tag{3.11}$$

where $|A|$ is the determinant and M_{ij} are the minors of the following matrix,

$$A = \begin{pmatrix} \Delta(q^2) & \Delta(bq) & \Delta(sq) & \Delta(\varepsilon q) \\ \Delta(qb) & \Delta(b^2) & \Delta(sb) & \Delta(\varepsilon b) \\ \Delta(qs) & \Delta(bs) & \Delta(s^2) & \Delta(\varepsilon s) \\ \Delta(q\varepsilon) & \Delta(b\varepsilon) & \Delta(s\varepsilon) & \Delta(\varepsilon^2) \end{pmatrix} \, , \tag{3.12}$$

with the elements, $\Delta(q^2) \equiv \sum_{\mathbf{p},j} q_j^2 v_{\mathbf{p},j}^2$, $\Delta(qb) \equiv \sum_{\mathbf{p},j} q_j b_j v_{\mathbf{p},j}^2$, $\Delta(q\varepsilon) \equiv \sum_{\mathbf{p},j} q_j \varepsilon_{\mathbf{p}j} v_{\mathbf{p},j}^2$, etc. The sum, $\sum_{\mathbf{p},j}$, means integration over momentum $\mathbf{p}$, and summation over all hadron-resonance species j contained in the model. The first term in the r.h.s. of Eq. (3.11) corresponds to the microscopic correlator (3.6) in the GCE. A nice feature of the microscopic correlator method is that particle number fluctuations and correlations in the MCE or CE, although being different from those in the GCE, are presented in terms of quantities calculated within the GCE. The microscopic correlator (3.11) can be used to calculate the primordial particle correlators in the MCE (or in the CE): $\langle \Delta N_{h_1} \Delta N_{h_2} \rangle_{m.c.e.} = \sum_{\mathbf{p},\mathbf{k}} \, \langle \Delta n_{\mathbf{p},h_1} \Delta n_{\mathbf{k},h_2} \rangle_{m.c.e.}$. An important point in the MCE (or CE), in comparison with the GCE, is a modification of the resonance decay contribution to fluctuations, Eq. (3.9). In the MCE it reads (see also Ref. [14] for the CE):

$$\begin{aligned} \langle \Delta N_i \Delta N_j \rangle_{m.c.e.} &= \langle \Delta N_i^* \Delta N_j^* \rangle_{m.c.e.} + \sum_R \langle N_R \rangle \langle \Delta n_i \Delta n_j \rangle_R + \sum_R \langle \Delta N_i^* \Delta N_R \rangle_{m.c.e.} \langle n_j \rangle_R \\ &+ \sum_R \langle \Delta N_j^* \Delta N_R \rangle_{m.c.e.} \langle n_i \rangle_R + \sum_{R,R'} \langle \Delta N_R \Delta N_{R'} \rangle_{m.c.e.} \langle n_i \rangle_R \langle n_j \rangle_{R'} \, . \end{aligned} \tag{3.13}$$

Additional terms in Eq. (3.13) compared to Eq. (3.9) are due to the correlations induced by exact energy and charge conservations in the MCE. The Eq. (3.13) has the same form in the CE, the

difference between these two ensembles appears when one specifies the microscopic correlators (3.11).

Mean hadron multiplicities in heavy ion collisions at high energies can be approximately fitted by the hadron-resonance gas model in the GCE. The fit parameters are temperature T, chemical potentials (μ_B, μ_S, μ_Q), and strangeness suppression factor γ_S, which allows for non-equilibrium strange hadron yields. There are several programs designed for the analysis of particle multiplicities in relativistic heavy-ion collisions within the hadron-resonance gas model, see e.g., SHARE [16], THERMUS [17] and THERMINATOR [18]. We use an extended version of the THERMUS model [17].

The dependence of μ_B on the c.m. energy will be parameterised as [3], $\mu_B\left(\sqrt{s_{NN}}\right) = 1.308\,\mathrm{GeV}\cdot(1+0.273\ \sqrt{s_{NN}})^{-1}$, where the c.m. nucleon-nucleon collision energy, $\sqrt{s_{NN}}$, is taken in GeV units. Furtheron we assume the system to be net strangeness free, $S = 0$, and to have the charge to baryon ratio of the initial colliding nuclei, $Q/B = 0.4$. For the chemical freeze-out condition we chose the average energy per particle $\langle E\rangle/\langle N\rangle = 1$ GeV [19]. Finally, in order to remove the remaining free parameter, γ_S, we use the parametrisation [4], $\gamma_S = 1 - 0.396\,\exp(-1.23\,T/\mu_B)$. This gives us five constraints for the five parameters of the model. The thermodynamical limit for the calculations of $\omega^{\pm}$ is assumed, thus volume V is not a parameter of our model calculations. The T and μ_B parameters at different collision energies are shown in Fig. 4.

The center of mass nucleon-nucleon energies, $\sqrt{s_{NN}}$, marked in the figures below correspond to the beam energies at SIS (2A GeV), AGS (11.6A GeV), SPS (20A, 30A, 40A, 80A, and 158A GeV), colliding energies at RHIC ($\sqrt{s_{NN}} = 62.4$ GeV, 130 GeV and 200 GeV) and LHC ($\sqrt{s_{NN}} = 5500$ GeV).

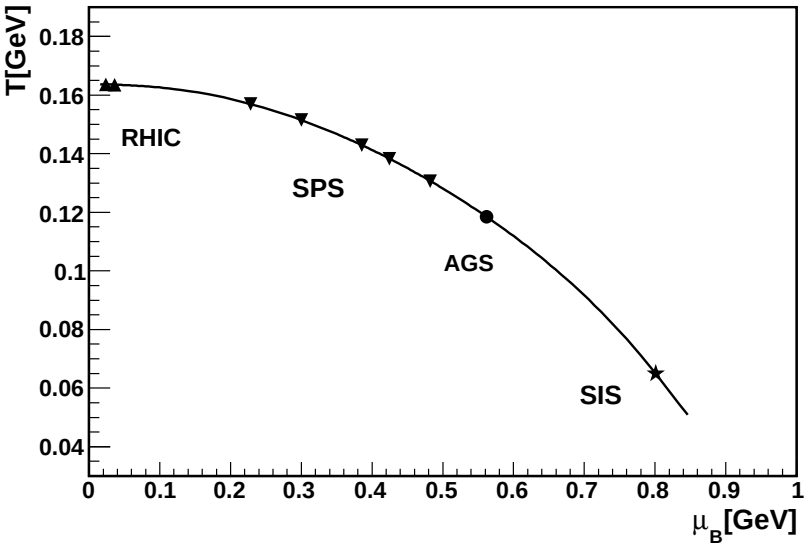

Figure 4: The chemical freeze-out line in central A+A collisions. See text for details.

The Fig. 5 shows the scaled variances for negatively charged particles, ω^-, and positively charged particles, ω^+, respectively, as a function of $\sqrt{s_{NN}}$. Our predictions will be compared with

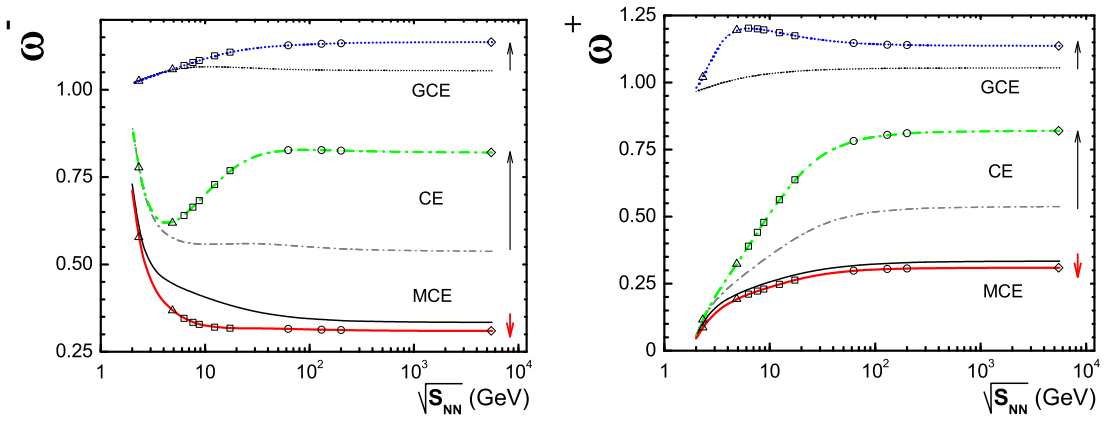

Figure 5: *Left.* The scaled variances for negatively charged particles, ω^-, both primordial and final, along the chemical freeze-out line for central Pb+Pb (Au+Au) collisions. Different lines present the GCE, CE, and MCE results. Symbols at the lines for final particles correspond to the specific collision energies. The T and μ_B values at these energies pointed out in Fig. 4. The arrows show the effect of resonance decays. *Right.* The same, but for ω^+.

the preliminary NA49 data on Pb+Pb collisions at 20*A*-158*A* GeV [20] with an approximately fixed number of projectile participants ranging from 190 to 200. This range corresponds to about 1% of all events.

The Fig. 5 corresponds to an ideal situation when all final hadrons are accepted by the detector. To compare our statistical model results with experimentally obtained values of $\omega^{\pm}$ the acceptance and resolution need to be taken into account. We neglect these momentum correlations between final hadrons. This is approximately valid for ω^+ and ω^-, as most decay channels only contain one positively (or negatively) charged particle, but much worse for ω^{ch}, due to decays of neutral resonances into two charged particles. This leads to:

$$\omega^{\pm} \;=\; 1 \,-\, q \,+\, q\,\omega^{\pm}_{4\pi}\,, \tag{3.14}$$

where $\omega^{\pm}_{4\pi}$ is a scaled variance calculated for all hadrons (measured by an ideal detector with full 4π-acceptance) and $\omega^{\pm}$ is the scaled variance measured by a real detector with a limited acceptance), q is the ratio between mean multiplicities of accepted and all hadrons. The Fig. 6 presents the scaled variances ω^- and ω^+ calculated with Eq. (3.14). The hadron-resonance gas calculations in the GCE, CE, and MCE shown in Fig. 5 are used for the $\omega^{\pm}_{4\pi}$. The NA49 acceptance used for the fluctuation measurements quoted here was located at about one rapidity unit above mid-rapidity (depending on collision energy). The Eq. (3.14) has the following property. If $\omega^{\pm}_{4\pi}$ is smaller or larger than 1, the same inequality remains to be valid for $\omega^{\pm}$ at any value of $0 < q \leq 1$. Due to this one finds a strong qualitative difference between the predictions of the statistical model valid for any freeze-out conditions and experimental acceptances: the CE and MCE correspond to $\omega^{\pm}_{m.c.e.} < \omega^{\pm}_{c.e.} < 1$, and the GCE to $\omega^{\pm}_{g.c.e.} > 1$.

From Fig. 6 it follows that the NA49 data for $\omega^{\pm}$ extracted from the most central Pb+Pb collisions at all SPS energies are most close to the results of the hadron-resonance gas statistical model within the MCE. The data reveal even stronger suppression of the particle number fluctuations. A

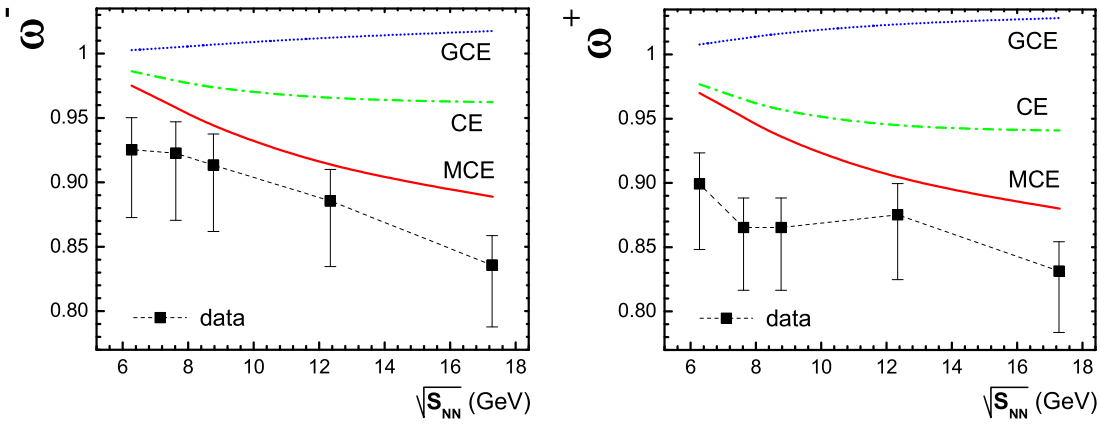

Figure 6: The scaled variances for negative (left) and positive (right) hadrons along the chemical freeze-out line for central Pb+Pb collisions at the SPS energies. The corresponding T and μ_B values at different SPS collision energies are presented in Fig. 4. Different lines show the GCE, CE, and MCE results calculated with the NA49 experimental acceptance according to Eq. (3.14).

possible reason of this is a suppression of particle number fluctuations due to the excluded volume effects in the hadron-resonance gas [21].

4. Summary and Outlook

It has been found that the fluctuations in the number of target participants strongly influences the multiplicity fluctuations. The consequences of this fact depend on the dynamics of the initial flows in A+A collisions. To study the genuine statistical fluctuations one needs to make the rigid event selection of about 1% of most central events.

The energy dependence of hadron multiplicity fluctuations in relativistic nucleus-nucleus collisions has been predicted in the statistical hadron-resonance gas model within the GCE, CE, and MCE formulations. The scaled variances of negatively, positively, and all charged particles for primordial and final state hadrons have been calculated at the chemical freeze-out in central Pb+Pb (Au+Au) collisions for different collision energies from SIS to LHC. A comparison with the preliminary NA49 data in Pb+Pb collisions at the SPS energies has been done for the samples of the most central collisions selected by the number of projectile participants. This selection allows to eliminate effect of fluctuations of the number of nucleon participants. The effect of the limited experimental acceptance was taken into account by use of the approximation valid for uncorrelated particles. The MCE results are most close to the measured scaled variances for positively and negatively charged particles. Even stronger suppression of the negative and positive particle number fluctuations seen in the data may be probably attributed to the excluded volume effects in the hadron-resonance gas [21]. Further study is needed to improve modelling of the effect of the limited experimental acceptance.

References

[1] H. Heiselberg, Phys. Rep. **351**, 161 (2001); S. Jeon and V. Koch, hep-ph/0304012, Review for Quark-Gluon Plasma 3, eds. R.C. Hwa and X.-N. Wang, World Scientific, Singapore, 430-490 (2004).

[2] H. Stöcker and W. Greiner, Phys. Rep. **137**, 277 (1986); J. Cleymans and H. Satz, Z. Phys. C **57**, 135 (1993); J. Sollfrank, M. Gaździcki, U. Heinz, and J. Rafelski, *ibid.* **61**, 659 (1994); G.D. Yen, M.I. Gorenstein, W. Greiner, and S.N. Yang, Phys. Rev. C **56**, 2210 (1997); F. Becattini, M. Gaździcki, and J. Solfrank, Eur. Phys. J. C **5**, 143 (1998); G.D. Yen and M.I. Gorenstein, Phys. Rev. C **59**, 2788 (1999); P. Braun-Munzinger, I. Heppe, and J. Stachel, Phys. Lett. B **465**, 15 (1999); P. Braun-Munzinger, D. Magestro, K. Redlich, and J. Stachel, *ibid.* **518**, 41(2001); F. Becattini, M. Gaździcki, A. Keränen, J. Mannienen, and R. Stock, Phys. Rev. C **69**, 024905 (2004); F. Becattini, J. Phys. Conf. Ser. **5**, 175 (2005). P. Braun-Munzinger, K. Redlich, and J. Stachel, nucl-th/0304013, Review for Quark Gluon Plasma 3, eds. R.C. Hwa and X.-N. Wang, World Scientific, Singapore, 491-599 (2004);

[3] J. Cleymans, H. Oeschler, K. Redlich, and S. Wheaton, Phys. Rev. C **73**, 034905 (2006).

[4] F. Becattini, J. Manninen, and M. Gaździcki, Phys. Rev. C **73**, 044905 (2006).

[5] I.N. Mishustin, Phys. Rev. Lett. **82**, 4779 (1999); Nucl. Phys. A **681**, 56c (2001); H. Heiselberg and A.D. Jackson, Phys. Rev. C **63**, 064904 (2001).

[6] M. Gaździcki, M.I. Gorenstein, and St. Mrówczyński, Phys. Lett. B **585**, 115 (2004); M.I. Gorenstein, M. Gaździcki, and O.S. Zozulya, *ibid.* **585**, 237 (2004).

[7] M.A. Stephanov, K. Rajagopal, and E.V. Shuryak, Phys. Rev. Lett. **81**, 4816 (1998); Phys. Rev. D **60**, 114028 (1999); M.A. Stephanov, Acta Phys. Polon. B **35**, 2939 (2004).

[8] S.V. Afanasev *et al*., [NA49 Collaboration], Phys. Rev. Lett. **86**, 1965 (2001); M.M. Aggarwal *et al*., [WA98 Collaboration], Phys. Rev. C **65**, 054912 (2002); J. Adams *et al*., [STAR Collaboration], Phys. Rev. C **69**, 044905 (2003); C. Roland *et al*., [NA49 Collaboration], J. Phys. G **30** S1381 (2004); Z.W. Chai *et al*., [PHOBOS Collaboration], J. Phys. Conf. Ser. **37**, 128 (2005).

[9] W. Ehehalt and W. Cassing, Nucl. Phys. A **602**, 449 (1996); W. Cassing and E.L. Bratkovskaya, Phys. Rep. **308**, 65 (1999).

[10] S.A. Bass et al., Prog. Part. Nucl. Phys.**41**, 255 (1998); M. Bleicher *et al.*, J. Phys. G **25**, 1859 (1999).

[11] V.P. Konchakovski, S. Haussler, M.I. Gorenstein, E.L. Bratkovskaya, M. Bleicher, and H. Stöcker, Phys. Rev. C **73**, 034902 (2006); V.P. Konchakovski, M.I. Gorenstein, E.L. Bratkovskaya, H. Stöcker, nucl-th/0606047.

[12] M. Gaździcki and M.I. Gorenstein, Phys. Lett. B **640**, 155 (2006).

[13] V.V. Begun, M. Gaździcki, M.I. Gorenstein, and O.S. Zozulya, Phys. Rev. C **70**, 034901 (2004); V.V. Begun, M.I. Gorenstein, and O.S. Zozulya, Phys. Rev. C **72**, 014902 (2005); A. Keränen, F. Becattini, V.V. Begun, M.I. Gorenstein, and O.S. Zozulya, J. Phys. G **31**, S1095 (2005); F. Becattini, A. Keränen, L. Ferroni, and T. Gabbriellini, Phys. Rev. C **72**, 064904 (2005); V.V. Begun, M.I. Gorenstein, A.P. Kostyuk, and O.S. Zozulya, Phys. Rev. C **71**, 054904 (2005); J. Cleymans, K. Redlich, and L. Turko, Phys. Rev. C **71**, 047902 (2005); J. Phys. G **31**, 1421 (2005); V.V. Begun, M.I. Gorenstein, A.P. Kostyuk, and O.S. Zozulya, J. Phys. G **32**, 935 (2006). V.V. Begun and M.I. Gorenstein, Phys. Rev. C **73**, 054904 (2006).

[14] V.V. Begun, M.I. Gorenstein, M. Hauer, V.P. Konchakovski, and O.S. Zozulya, Phys. Rev. C **74**, 044903 (2006).

[15] S. Jeon and V. Koch, Phys. Rev. Lett. **83**, 5435 (1999).

[16] G. Torrieri, S. Steinke, W. Broniowski, W. Florkowski, J. Letessier, and J. Rafelski, Comput. Phys. Commun. **167**, 229 (2005).

[17] S. Wheaton and J. Cleymans, J. Phys. G **31** 1069 (2005)

[18] A. Kisiel, T. Taluc, W. Broniowski, and W. Florkowski, Comput. Phys. Commun. **174**, 669 (2006).

[19] J. Cleymans and K. Redlich, Phys. Rev. Lett. **81**, 5284 (1998).

[20] B. Lungwitz *et al*., [NA49 Collaboration], Proceedings of "Correlations and Fluctuations in Relativistic Nuclear Collisions", July 7-9, 2006, Florence, Italy.

[21] M.I. Gorenstein, M. Hauer, and D. Nikolajenko, in preparation.